AUTHOR QUERY FORM

AIP Publishing	**Journal: J. Chem. Phys.** **Article Number: JCP21-AR-03495**	**Please provide your responses and any corrections by annotating this PDF and uploading it to AIP's eProof website as detailed in the Welcome email.**

Dear Author,

Below are the queries associated with your article. Please answer all of these queries before sending the proof back to AIP.

Article checklist: In order to ensure greater accuracy, please check the following and make all necessary corrections before returning your proof.
1. Is the title of your article accurate and spelled correctly?
2. Please check affiliations including spelling, completeness, and correct linking to authors.
3. Did you remember to include acknowledgment of funding, if required, and is it accurate?

Location in article	Query/Remark: click on the Q link to navigate to the appropriate spot in the proof. There, insert your comments as a PDF annotation.
Q1	Please check that the author names are in the proper order and spelled correctly. Also, please ensure that each author's given and surnames have been correctly identified (given names are highlighted in red and surnames appear in blue).
Q2	In the sentence beginning "The analysis of. . .," please confirm that "the next section" refers to Sec. III.
Q3	In the sentence beginning "During the analysis. . .," please confirm that "the next section" refers to Sec. III.
Q4	In the sentence beginning "Figure 6 also shows...," please verify that "the latter figure..." refers to Figure 6.
Q5	Please reword the sentence beginning with "It is worth..." so that your meaning will be clear to the reader.
Q6	The journal requires a Conflict of Interest statement. Please provide text explaining any potential conflicts of interest or state that you have no conflicts of interest to disclose.
Q7	Please confirm the change in author's initials in Refs. 23 and 44.
Q8	Please confirm the change in page number in Ref. 29.
Q9	We were unable to locate a digital object identifier (doi) for Refs. 46 and 51. Please verify and correct author names and journal details (journal title, volume number, page number, and year) as needed and provide the doi. If a doi is not available, no other information is needed from you. For additional information on doi's, please select this link: http//www.doi.org/.
Q10	Please provide author group in Ref. 48.
	Please confirm ORCIDs are accurate. If you wish to add an ORCID for any author that does not have one, you may do so now. For more information on ORCID, see https://orcid.org/. Federico Palazzetti – 0000-0002-1361-0524 David Cappelletti – 0000-0002-9652-2457 Cecilia Coletti – 0000-0002-3609-290X Stefano Falcinelli – 0000-0002-5301-6730 Fernando Pirani –
	Please check and confirm the Funder(s) and Grant Reference Number(s) provided with your submission: Ministero dell'Istruzione, dell'Università della Ricerca, Award/Contract Number RBSI14U3VF Please add any additional funding sources not stated above.

Thank you for your assistance.

Author Proof

The Journal of Chemical Physics ARTICLE scitation.org/journal/jcp

Molecular beam scattering experiments on noble gas–propylene oxide: Total integral cross sections and potential energy surfaces of He– and Ne–C_3H_6O

Cite as: J. Chem. Phys. 155, 000000 (2021); doi: 10.1063/5.0073737
Submitted: 3 October 2021 • Accepted: 27 November 2021 •
Published Online: 9 99 9999

View Online Export Citation CrossMark

Federico Palazzetti,[1,a)] David Cappelletti,[1] Cecilia Coletti,[2] Stefano Falcinelli,[3] and Fernando Pirani[1,3]

AFFILIATIONS

[1] Dipartimento di Chimica, Biologia e Biotecnologie – Università degli Studi di Perugia, Perugia, Italy
[2] Dipartimento di Farmacia, Università degli Studi "G. D'Annunzio" Chieti-Pescara, Chieti, Italy
[3] Dipartimento di Ingegneria Civile ed Ambientale, Università degli Studi di Perugia, Perugia, Italy

[a)] **Author to whom correspondence should be addressed:** federicopalazzetti@yahoo.it

ABSTRACT

The interactions of He and Ne with propylene oxide have been investigated with the molecular beam technique by measuring the total (elastic + inelastic) integral cross section as a function of collision velocity. Starting from the analysis of these experimental data, potential energy surfaces, formulated as a function of the separation distance and orientation of propylene oxide with respect to the interacting partners, have been built: The average depth of potential wells (located at intermediate separation distances) has been characterized by analyzing the observed "glory" quantum effects, and the strength of long-range attractions has been obtained from the magnitude and the velocity dependence of the smooth component of measured cross sections. The surfaces, tested and improved against new *ab initio* calculations of minima interaction energies at the complete basis set level of theory, are defined in the full space of relative configurations. This represents a crucial condition to provide force fields useful to carry out, in general, important molecular property simulations and to evaluate, in the present case, the spectroscopic features and the dynamical selectivity of weakly bound complexes formed by propylene oxide, a prototype chiral species, during collisions in interstellar clouds and winds, in the space and planetary atmospheres. The adopted formulation of the interaction can be readily extended to similar systems, involving heavier noble gases or diatomic molecules (H_2, O_2, and N_2) as well as to propylene oxide dimers.

Published under an exclusive license by AIP Publishing. https://doi.org/10.1063/5.0073737

I. INTRODUCTION

The study of the intermolecular interactions of a polyatomic molecule with atoms and simple diatomic species is of crucial relevance in many research fields since it permits the evaluation of spectroscopic and dynamical features of systems of increasing complexity formed via collisions in many gaseous environments of interest. The characterization of multidimensional potential energy surfaces (PESs), determined by anisotropic non-covalent interactions defining in detail structure and energetics of weakly bound adducts, is a topic of general interest because PESs control the formation of the precursor states of several basic elementary processes. The involved weak intermolecular forces ultimately determine the collision dynamics in *cold environments*, as interstellar media (ISM), planetary atmospheres, and vortices, as well as in *hot environments*, as flames and plasmas, but they can hardly be characterized by standard methods. In this work, we focus on the interaction between propylene oxide and the lightest rare gas atoms, helium and neon. Propylene oxide is one of the simplest chiral molecules and was detected in ISM.[1] This finding stimulated the research toward the detection of possible enantiomeric excess in the universe[2] and the emergence of chiral selectivity in nature,[3] a very much debated topic.[4,5]

The structure of propylene oxide was initially characterized by microwave spectroscopy,[6,7] and its chiroptical properties were investigated experimentally[8] by vibrational circular dichroism and

Author Proof

Published under an exclusive license by AIP Publishing

Raman optical activity spectra[9] and by *ab initio* calculations.[10] In view of possible applications in experimental dynamics studies, molecular beams (MBs) of propylene oxide were rotationally state-selected and aligned by an electrostatic hexapole.[11,12] More recently, synchrotron radiation has been used to measure the double ionization threshold[13] and the angular distribution of products[14] from various dissociation channels of the gas-phase molecules. Quantum mechanical approaches have also been employed to characterize the structural isomers of propylene oxide and their interconversion pathways and chirality changing mechanisms.[15,16]

The discovery of propylene oxide in the interstellar cold gas environment also stimulated investigations on the interaction of this molecule with those partners commonly found in ISM and up to date information on such topic is rather limited. Helium is the second most abundant element in ISM, after hydrogen; neon and argon are also among the most abundant elements, and from the chemical point of view, they are even more interesting than helium since they are more likely to react (see Ref. 17 and the references therein). In non-local thermal equilibrium conditions, such as those often found in space, the abundance of all chemical species is strongly determined by collisional and radiative processes, for which state-to-state rate coefficients need to be accurately known to model the system and reproduce the evolutionary processes. For this purpose, detailed PESs describing the interaction of propylene oxide with molecular hydrogen and helium and other neutral molecules, such as N_2 and O_2,[18] are needed. Note that such interaction potentials should be able to describe all the main features of the weakly bound adducts which might form between propylene oxide and the colliding partner as well as the long-range attraction regions which are emerging as important driving forces to determine the capture and outcome of the various collisional processes. On the other hand, accurate experimental data probing in detail the structure and binding energy of the collisional adducts or complexes are essential to assess the validity of the proposed interaction potentials.

As stressed above, in the case of propylene oxide, only limited information on the intermolecular interactions is currently available: Rotational spectroscopy has been employed to characterize the structure and binding energy of the complexes with Ne,[19] Ar,[20] and Kr[21] and of the homochiral and heterochiral forms of propylene oxide dimers.[22] Recently, Faure *et al.*[23] calculated the first quantum scattering cross sections for the rotational excitation of rigid propylene oxide upon collision with helium. To this aim, a PES fitted on CCSD(T)-F12b points extrapolated to the complete basis set limit was also obtained. The PES was then refitted with an expansion into spherical harmonics to perform the quantum dynamical calculations. Such a procedure, however, together with the number of coupled channels and the basis functions needed to reach convergence, can easily become computationally prohibitive.

One of the issues related to the construction and use of *ab initio* based PESs for non-covalently interacting systems is the need to use a very high level of theory to reach the desired accuracy and the proper representation of the long-range regions of each PES, which, as mentioned before, can be determinant for the evolution of the dynamics.[24,25] For the interaction of helium–neutral molecules and molecular ions, some numerical oscillations at a long range, for which the use of large auxiliary bases is needed, were indeed reported.[26,27] Furthermore, the accurate description of the wide long-range region requires a very large number of *ab initio* points together with robust interpolation procedures. Such computational load is expected to grow larger when considering heavier rare gas atoms and complex polyatomic molecules.

In the present article, we report for the first time a molecular beam experimental study addressed to measure the total (elastic + inelastic) integral cross section, for the scattering of He and Ne by propylene oxide, as a function of collision velocity, selected in the thermal interval. These measurements, performed under high angular and velocity resolution conditions, permitted to resolve quantum "glory" interference effects, observable as oscillating patterns in the velocity dependence of the cross section. The experimental findings provide information on the absolute scale of the long-range attraction and of the average binding energy in the range of equilibrium distances. A parallel effort has been addressed to the development of an integrated phenomenological-theoretical method, applied to characterize the range and strength of the interaction as a function of the separation distance and relative orientation of He, Ne–rigid propylene oxide partners. Such a method allowed for the attainment of the full PES for these systems in an analytical form, formulated in terms of parameters related to fundamental physical properties of the interacting partners. The potentials were refined and tested against the experimental cross section data and the results of *ab initio* calculations of the minimum energy points of the surfaces performed at the CCSD(T)/CBS level of theory. The adopted procedure provides PESs properly formulated in the full space of the relative configurations of involved partners, and this is a crucial condition to carry out any type of molecular dynamics simulation under several conditions of interest.

In the case of He–propylene oxide, the identified PES minima lie very close to the four found in Ref. 23; however, an additional one is predicted by our model and confirmed by the present *ab initio* calculations. Five minimum configurations also characterize the PES of the Ne–propylene oxide system, for which no previous representation of the full interaction potential is available. The new PESs are computationally fast to achieve and can therefore be profitably used to describe scattering processes through molecular dynamics studies, in this case particularly relevant for the evaluation of possible chiral effects.[28] Note that the same methodology can be straightforwardly extended to characterize the interaction potential between propylene oxide and heavier noble gas atoms (Ng), as well as that for propylene oxide–propylene oxide interactions, a system of crucial interest because it would enable the observation of possible different dynamical effects arising in homochiral and heterochiral dimers.[29]

II. EXPERIMENTAL DETAILS

Experiments have been carried out in the gas phase with the molecular beam (MB) technique. High resolution single collision conditions are realized, useful to measure the velocity (v) dependence of the total (elastic + inelastic) integral cross section Q.[30,31]

The experiments have been performed with a MB apparatus that has been extensively described previously,[32] and in the recent years, it has been used to investigate weak hydrogen and halogen

Author Proof

Published under an exclusive license by AIP Publishing

intermolecular bonds.[33–35] In synthesis, the apparatus is composed of a set of differentially pumped vacuum chambers. The MB, here formed by He/Ne atoms, is generated by the gas expansion from a nozzle, maintaining the temperature in the range of 77–600 K and the total pressure in the source within 7–20 mbar in order to avoid cluster formation and to cover a wide range of collision velocity. Under such conditions, the MB emerges with near effusive or moderate supersonic character and is analyzed in velocity by a mechanical selector, composed of six slotted disks. After a proper collimation, the MB collides at a "nominal" velocity v with the stationary target gas (propylene oxide) contained in the scattering chamber at a pressure not larger than 3×10^{-4} mbar to assure the occurrence of single collision events. The chamber is kept at room temperature to avoid condensation effects of the propylene oxide on the walls and to maintain the rotational temperature (T = 300 K) of the target molecules sufficiently high to determine an average molecular rotation time comparable with the collision time. The latter condition is critical to limit anisotropy effects in the scattering and then to better resolve, at least in He–propylene oxide collisions, frequency and amplitude of the "glory" oscillatory pattern (see below).

The MB is detected downstream by a quadrupole mass spectrometer, coupled with an ion-counting device. At each selected velocity v of the projectile atoms, the quantity to be measured is the MB attenuation I/I_0, where I represents the MB intensity detected with the target in the scattering chamber (filled at the chosen pressure) and I_0 is the MB intensity measured with the scattering chamber empty. From the measurement of the ratio I/I_0, it is possible to determine the value of the integral cross section $Q(v)$ by the Lambert–Beer law: Calibration methodology and reference data are given in Refs. 36–38.

The availability of projectiles (here He and Ne) in a large speed range has been of great relevance to perform measurements in a sufficiently extended interval of v. The choice of the heavier propylene oxide as the target, confined in a box at a defined pressure and temperature, has been crucial to carry out high angular and velocity resolution experiments. In particular, the use of the lighter He and Ne atoms in the beams, and the heavier propylene oxide molecules in the scattering chamber, increases the limiting angle, imposed by the indetermination principle, and reduces the random thermal motion of the target.[32] This choice determines proper conditions to resolve quantum "glory" interference effects, observable as oscillations overimposed to a smooth component in the $Q(v)$ dependence. The collected experimental $Q(v)$ results probe in detail, and in an internally consistent way, the absolute scale of the interaction at both long and intermediate distance ranges.[30–32]

The experimental results are reported in Figs. 1 and 2, where measured cross sections are plotted as $Q(v) \cdot v^{2/5}$ to emphasize the "glory" quantum interference,[31] which appears to exhibit a small amplitude in both cases.[30,31] Moreover, the He, Ne–propylene oxide systems exhibit a completely different behavior of the observables, thus revealing significant variations in the intermolecular interactions, which drive the dynamics of single collision events.

The analysis of $Q(v)$ (see Sec. III) provided a quantitative characterization of the strength of the average intermolecular interaction both at a long range, obtained from the velocity dependence of the average value of $Q(v)$, and in the potential well region, probed by the resolved glory structure.[30–36] During the analysis, Center-of-Mass (CM) cross section values have been calculated within the semi-classical Jeffreys–Wentzel–Kramers–Brillouin approximation[39] from the assumed intermolecular interaction potential V (see

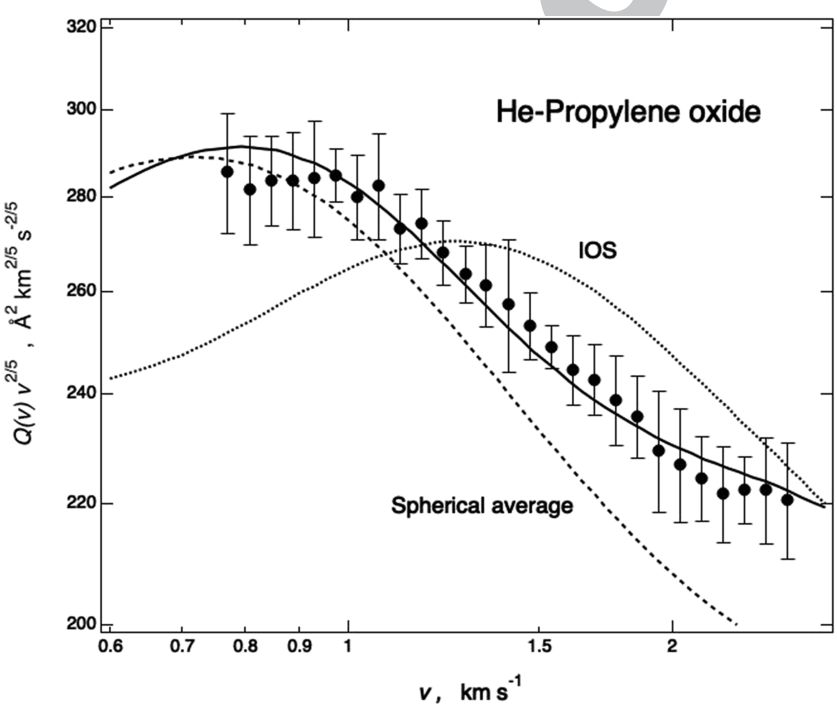

FIG. 1. Experimental integral cross sections Q (black points with vertical error bars) as a function of the selected beam velocity v (reported in logarithmic scale to better define the glory maximum position[30–32]) for He–propylene oxide. The curves represent the cross sections calculated on the present PES according to three different regimes: in conditions of isotropic (spherical) interaction (dashed line), in conditions of anisotropic interaction according to the Infinite Order Sudden (IOS) approximation (dotted line), and through a combined data analysis, smoothly switching from the isotropic (holding for lower v values) to anisotropic (holding for higher v values) interactions (full line).

Published under an exclusive license by AIP Publishing

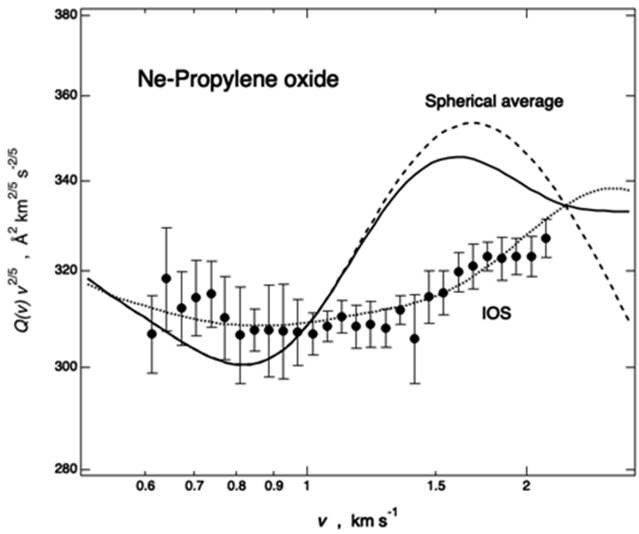

FIG. 2. Experimental integral cross sections Q (black points with vertical error bars) as a function of the selected beam velocity v (reported in logarithmic scale to better define the glory extreme positions[30–32]) for Ne–propylene oxide. The curves represent the cross sections calculated on the present PES according to three different regimes: in conditions of isotropic (spherical) interaction (dashed line), in conditions of anisotropic interaction according to the IOS approximation (dotted line), and through a combined data analysis, smoothly switching from the isotropic (holding for lower v values) to anisotropic (holding for higher v values) interactions (full line).

Sec. III) and afterward convoluted in the laboratory frame to make a direct comparison with the measured $Q(v)$.[32] The trial-and-error procedure has been adopted, and the potential parameters, defining the basic features of V, have been tested and fine-tuned to obtain the best comparison between experimental and calculated data.

III. POTENTIAL ENERGY SURFACES

A. The improved Lennard-Jones potential

A pairwise additivity approach has been adopted to provide an analytical formulation of the intermolecular potential. The total interaction potential V has been defined as a sum of Improved Lennard-Jones (ILJ) potential pair-contributions, each one involving the noble gas atom (Ng = He, Ne) and one of the seven centers distributed in the propylene oxide, C_3H_6O, molecular frame. We selected as the most representative propylene oxide interaction centers the asymmetric carbon C, the C atom of the CH_2 group, the three hydrogen H atoms of CH and CH_2 groups, the oxygen atom O, and the methyl group CH_3, considered as a structureless partner, i.e., as a sphere having the mass of the methyl group, centered on the carbon atom.

For each interacting pair, the ILJ contribution $V(r)$ is expressed as follows:[31]

$$V(r) = \varepsilon\left(\frac{m}{n(r)-m}\left(\frac{r_m}{r}\right)^{n(r)} - \frac{n(r)}{n(r)-m}\left(\frac{r_m}{r}\right)^{m}\right),$$

where r is the Ng–individual center (or Ng–effective atom) distance, ε and r_m are the potential well depth and equilibrium distance, respectively, associated with the considered pair, while r/r_m is the reduced distance. For neutral–neutral pairs, the parameter m is 6. The $n(r)$ term is given[31] by

$$n(r) = \beta + 4\left(\frac{r}{r_m}\right)^2,$$

where β is a parameter related to the hardness of the two interacting species, and for the present systems, its value is comprised between 7.5 and 8.5.

The nature of the intermolecular potential in the present systems is essentially of the van der Waals type: The involved PESs are determined by the critical balance of size repulsion and dispersion attraction. The zero-order values of the van der Waals interaction parameters have been estimated by the polarizabilities of the interacting partners[42,43] identified here with Ng–CH_3, Ng–C, Ng–O, and Ng–H pairs. In particular, the polarizability of He and Ne amounts to 0.20 and 0.40 Å^3, respectively,[42,44] while that of propylene oxide, 6.2 Å^3, has been decomposed in partial contributions, corresponding to 2.10, 1.10, 0.80, and 0.35 Å^3 due to CH_3, C, O, and H partners, respectively. Note that C, H, and O are considered effective atomic centers since their polarizabilities are different from those of isolated gas-phase atoms. Such zero-order values of the potential parameters, indirectly including the small effect of induction contribution, have been fine-tuned to reproduce measured $Q(v)$ data and against *ab initio* calculations (Sec. III C) for He–propylene oxide. Their optimized values have been simply scaled for the different Ne polarizabilities to build the PES for Ne–propylene oxide, which was again tested against the corresponding experimental $Q(v)$ data and *ab initio* calculations. For He– and Ne–propylene oxide, the values of the obtained parameters defining the PESs have been reported in Tables I and II, respectively.

B. Cross-sectional analysis and potential parametrization

The dynamical treatment used for the data analysis exploits the comparison between the energy barriers, preliminarily evaluated at a fixed intermolecular distance and associated with the orbiting motion of Ng around the propylene oxide molecule, with the average rotational energy of propylene oxide given by RT, where T is the temperature and R, the gas constant, amounts to $8.614 \cdot 10^{-2}$ meV K^{-1}.

TABLE I. Parameters, equilibrium distance r_m, and well depth ε used in the improved Lennard-Jones model to describe the interaction pair individual contributions in the He–propylene oxide system. The parameter β has been taken in the range of values typical of van der Waals interactions.[31,40,41]

	Well depth (meV)	Equilibrium distance (Å)	β
CH_3–He	1.75	3.81	7.5
C–He	1.76	3.45	7.5
O–He	2.83	3.14	7.5
H–He	1.32	2.93	8.5

Author Proof

Published under an exclusive license by AIP Publishing

TABLE II. Parameters, equilibrium distance r_m, and well depth ε used in the improved Lennard-Jones model to describe the interaction pair individual contributions in the Ne–propylene oxide system. The parameter β has been taken in the range of values typical of van der Waals interactions.[31,40,41]

	Well depth (meV)	Equilibrium distance (Å)	β
CH_3–Ne	3.73	3.83	7.5
C–Ne	3.47	3.51	7.5
O–Ne	5.27	3.24	7.5
H–Ne	2.19	3.07	8.5

For He–propylene oxide, the predicted energy barriers are lower than RT at the experimental temperature T = 300 K, even in the potential well region. They are thus expected to be sufficiently low to reduce, or even eliminate, the trapping of the colliding system into rigid configurations (see Sec. IV). In such conditions, the long interaction time associated with slow collisions favors a dynamical behavior driven by the partial or total orientation averaging of the involved interaction. Therefore, measured cross sections have been analyzed assuming that the scattering at low v is driven by an effective central field potential, while at high v the collision time reduces, and the anisotropic behavior of the PES increases its effect, permitting a more direct control of the collision dynamics, since the molecules are seen under sudden conditions by the fast projectile atoms. Consequently, the analysis of the cross sections at the lowest investigated v has been performed adopting an effective isotropic interaction, identified with the spherical average of the PES. On the other hand, at the highest investigated v, the reduced collision time suggests that the Infinite Order Sudden Approximation (IOSA) is more appropriate for the cross-sectional simulations. The switch between the two regimes, operative at intermediate velocities, has been performed by using a weighted sum, depending on v, of the two types of calculations, providing an excellent comparison with the scattering experimental data in the whole range of probed v (Fig. 1). The same treatment has been successfully applied to other atom–molecule systems (see, for instance, Refs. 33 and 45 and the references therein, where major details on the different collisional regimes and on their weighted sum are given). Note that for less anisotropic cases involving rotationally hot molecules (at higher T), a simple isotropic potential drives the collisions in the full range of the investigated v.[46,47]

For Ne–propylene oxide, the energy barriers in the potential well region, predicted by the extended potential formulation, are comparable with RT at 300 K (see also Sec. IV), and therefore, the IOSA has been adopted to test the PES reliability on the experimental data in the whole range of investigated v values and is shown (Fig. 2) to correctly reproduce the behavior of experimental cross sections.

C. *Ab initio* calculations

Calculations were performed using MP2 and CCSD(T) levels of theory with Gaussian09[48] to obtain minimum geometries and binding energies for He– and Ne–propylene oxide complexes. For both systems, the initial structures to submit to the minimization process were taken as the minima obtained by the analytical ILJ PESs. A preliminary optimization, where the positions of the hydrogen atoms of the methyl group of propylene oxide are considered flexible, was carried out at the MP2/aug-cc-pVDZ level of theory for each starting structure. This is needed to identify the orientation of the methyl group, treated as a pseudo-atom in the analytical PES. Optimizations of He–propylene oxide, where the propylene oxide moiety is considered rigid, were then carried out at MP2/aug-cc-pVnZ (n = 3,4,5) to extrapolate the complete basis set limit by using a mixed exponential/Gaussian function.[49] The CCSD(T) complete basis set limit energy for the complexes, $E^{CBS}_{CCSD(T)}$, was evaluated using the MP2 complete basis set limit, E^{CBS}_{MP2}, considering that $E^{CBS}_{CCSD(T)} \approx E^{CBS}_{MP2} + \Delta CCSD(T)$, where the CCSD(T) correction to the MP2 energy, $\Delta CCSD(T) = E^{aug-cc-pVTZ}_{CCSD(T)} - E^{aug-cc-pVTZ}_{MP2}$, was here calculated with the aug-cc-pVTZ basis set. As a matter of fact, for many weakly bound adducts, it was noted that the higher order correlation effects are only slightly sensitive to the size of the basis set, provided that diffuse functions are included, and the basis is not too small.[50] $E^{aug-cc-pVTZ}_{CCSD(T)}$ was obtained as a single point calculation on the geometry optimized at the MP2/aug-cc-pVTZ level of theory.

For Ne–propylene oxide, the same optimization procedure was followed, although the larger number of electrons only allowed us to calculate the CCSD(T) correction by the aug-cc-pVDZ basis set, i.e., $\Delta CCSD(T) = E^{aug-cc-pVDZ}_{CCSD(T)} - E^{aug-cc-pVDZ}_{MP2}$.

IV. RESULTS AND DISCUSSION

The PESs of both systems are characterized by five minima, whose geometry is reported in Table III for the He– propylene oxide system and in Table IV for the Ne–propylene oxide system according to the reference frame depicted in Fig. 3: The system is embedded in a *xyz* Cartesian reference frame, where the x, y, and z axes correspond to the principal molecular axes of inertia b, c, and a, respectively[23] and the origin is the center of mass of the molecule. The position of the noble gas with respect to propylene oxide is expressed in spherical coordinates R, θ and ϕ, where R is the distance between the noble gas and the center of mass of the molecule, and θ and ϕ are the polar angles.

Figure 4 depicts the five minima position for He–propylene oxide, provided by the present ILJ PES; the corresponding coordinates and interaction energies are reported in Table III together with those obtained by the present *ab initio* calculations at the CCSD(T)/CBS level of theory (the binding energies evaluated at each level of theory are reported in Table S1 of the supplementary material) and by the *ab initio* PES from Ref. 23. We note here that the small differences (less than 0.5 meV in energy and 0.09 Å in distance) between the present and *ab initio* values from Ref. 23, calculated with a very similar, but not identical, level of theory might as well be due to the different orientation of the methyl group considered in the two types of calculations.

The interaction energies of the five minima characterizing the PES of helium–propylene oxide are comprised between −9.79 and −7.62 meV, with the global minimum remarkably close in geometry and energy to the present and *ab initio* values of Ref. 23. In such configuration, the helium atom mainly interacts with the oxygen

Author Proof

Published under an exclusive license by AIP Publishing

TABLE III. Minimum geometries and potential energy for He–propylene oxide interactions obtained by the ILJ PES (bold), by the present *ab initio* calculations, and by the *ab initio* calculations of Faure *et al.*[23] (parentheses).

	Minimum 1	Minimum 2	Minimum 3	Minimum 4	Minimum 5
Θ	**49.4**	**90.4**	**91.6**	**62.9**	**32.6**
	49.3 (50.0)	104.1 (102.0)	100.9 (100.0)	77.2	25.1 (26.3)
Φ	**110.4**	**36.7**	**148.6**	**256.1**	**256.5**
	104.1 (104.0)	26.5 (1.7)	153.1 (154.0)	252.4	254.0 (245.9)
R (Å)	**3.591**	**3.614**	**3.503**	**3.550**	**3.894**
	3.528 (3.493)	3.675 (3.605)	3.357 (3.356)	3.564	3.844 (3.935)
V (meV)	**−9.79**	**−8.54**	**−8.49**	**−8.28**	**−7.62**
	−9.67 (−9.72)	−6.47 (−6.38)	−8.91 (−8.45)	−6.79	−7.10 (−6.86)

TABLE IV. Minimum geometries and potential for Ne–propylene oxide interactions obtained by the present PES (bold) and by the present *ab initio* calculations.

	Minimum 1	Minimum 2	Minimum 3	Minimum 4	Minimum 5
θ	**49.4**	**83.8**	**93.9**	**95.2**	**35.4**
	50.8	83.1	103.0	101.8	29.1
ϕ	**111.0**	**256.3**	**31.1**	**151.7**	**255.7**
	103.0	252.3	3.2	154.2	256.9
R (Å)	**3.697**	**3.426**	**3.660**	**3.573**	**3.948**
	3.659	3.490	3.600	3.396	3.904
V (meV)	**−18.05**	**−17.64**	**−16.62**	**−16.27**	**−14.47**
	−17.44	−13.48	−15.51	−18.37	−14.31

and the chiral carbon atom of the ring in a perpendicular fashion. The other four minima also show a very similar geometry to the *ab initio* determinations, although the sequence of their interaction energies does not always follow the same order, with the ILJ values generally providing slightly deeper minima. It has to be noted, however, that such discrepancies are well within 2 meV, much smaller than the accuracy of *ab initio* determinations. Because of this and because the binding energies of all minima lie very close, as might be expected from the nature of van der Waals interactions in the present system, the ranking of the well depths can be easily different according to the various approaches. The ILJ potential and the present *ab initio* calculations identify five minima on the PES,

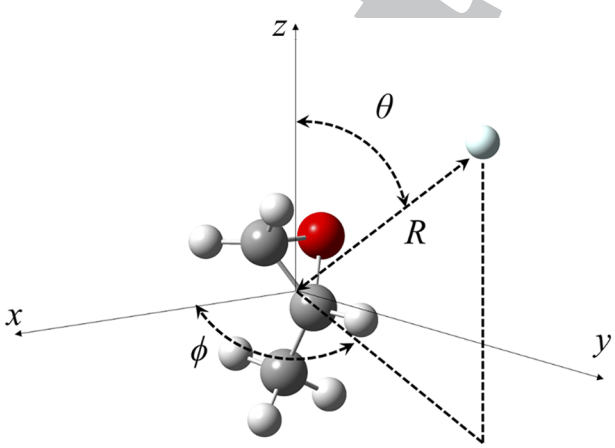

FIG. 3. Coordinate frame for the rare gas– propylene oxide system.

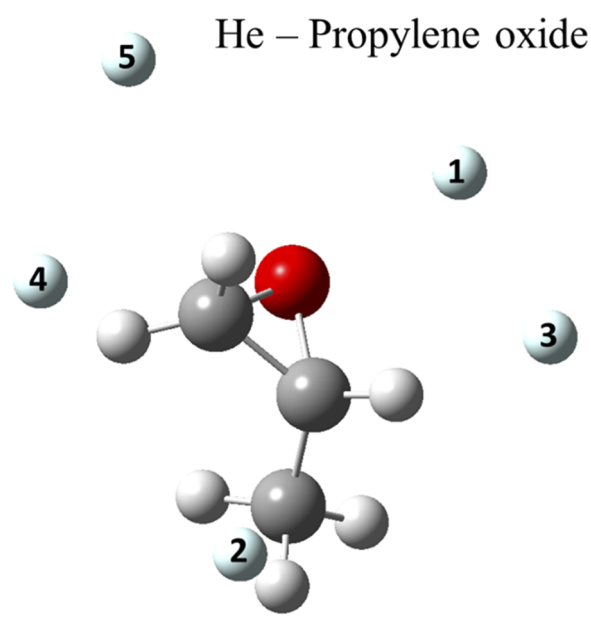

FIG. 4. Minimum geometries for He–propylene oxide identified on the ILJ PES. The numbering of the He atom corresponds to the minima reported in Table III.

Author Proof

Published under an exclusive license by AIP Publishing

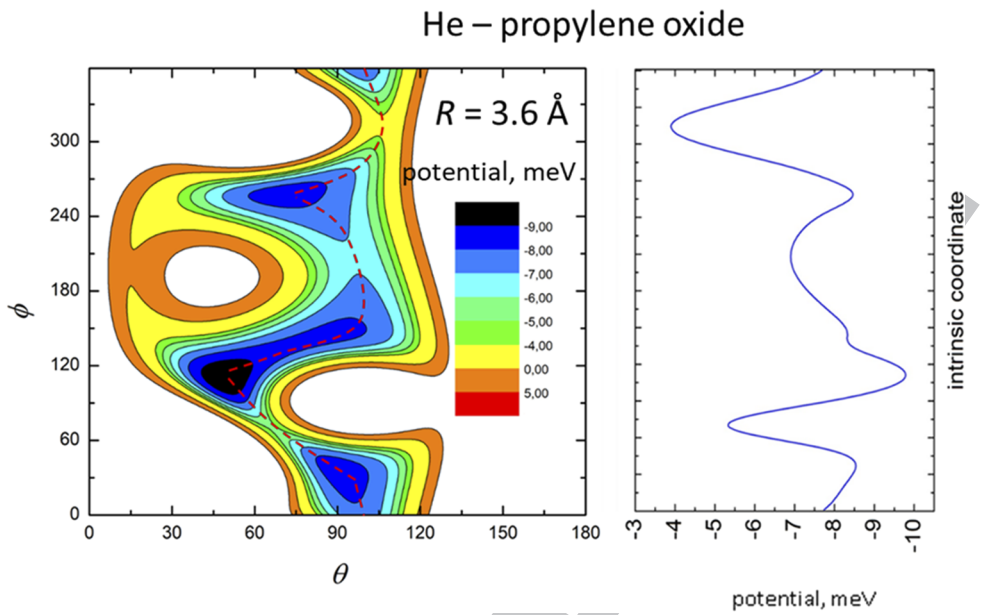

FIG. 5. The left panel shows the color contour map for the He–propylene oxide system at R = 3.6 Å. The axes report the angles θ and ϕ in degrees, while a color scale reports the potential energy in meV. The red dashed line indicates the minimum energy path. The right panel shows the energy profile of the minimum energy path.

whereas Ref. 23 only reports four. The fifth minimum (here minimum 4) is determined by the interaction of the helium atom with the CH_2 group and, in part, with the propylene oxide oxygen, in a similar fashion to minimum 5, as shown by the very close value of the angle ϕ.

Figures 5 and 6 show the contour maps of He–propylene oxide PES at R equal to 3.6 and 4.0 Å, respectively, and indicate that while ϕ can fully range from 0° to 360°, the variation interval of θ is much more restricted, with repulsive contributions being predominant, for instance, in the region with $\theta > 140°$. Furthermore, the minima can

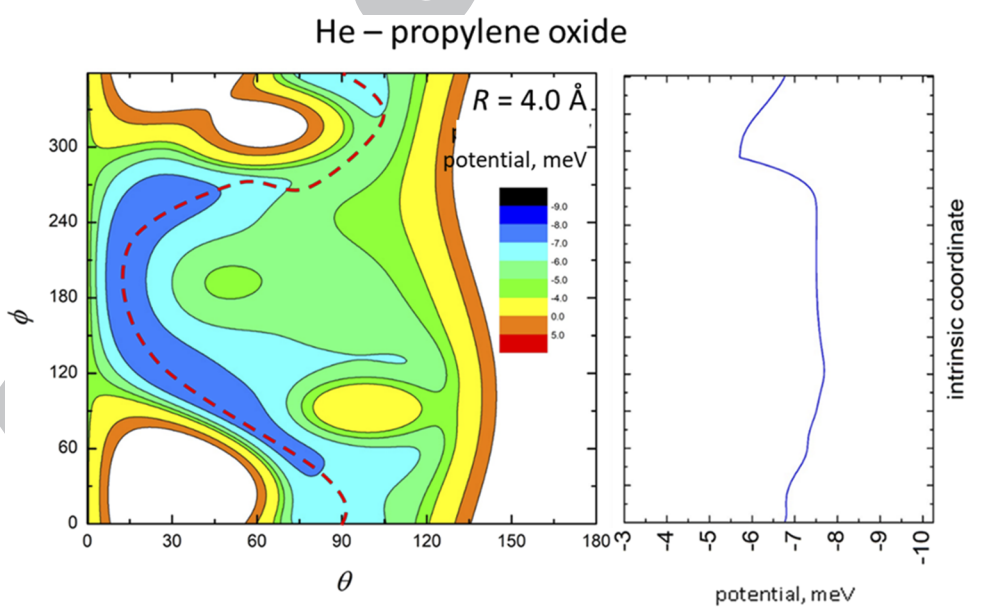

FIG. 6. The left panel shows the color contour map for the He–propylene oxide system at R = 4.0 Å. The axes report the angles θ and ϕ in degrees, while a color scale indicates the potential energy in meV. The red dashed line indicates the minimum energy path. The right panel shows the energy profile of the minimum energy path.

Published under an exclusive license by AIP Publishing

nearly always be found around the oxirane ring at values 50° < θ < 100°, as also shown in the energy profiles reported in Fig. S1 of the supplementary material. Figures 5 and 6 also report the minimum energy path (MEP), plotted as a red dashed line on the contour maps and, more clearly, in the right panels. The MEP helps to estimate the smallest barriers between the minima configurations of the collision complex and thus provides information on the possibility of interconversion between them at the considered temperature. Their values, as mentioned in Sec. III, can indeed be compared to the rotation energy RT available for the revolution of He around the propylene oxide molecule. The MEP at R = 3.6 Å (Fig. 5) shows three barriers whose height is ca. 4–5 meV, thus much lower than RT, and that for T = 300 K, corresponding to the present experimental conditions, it amounts to 25.8 meV, therefore allowing an almost free revolution of He around the propylene oxide molecule during slow collisions at room temperature. In contrast, in cold and ultracold regimes as those found in the ISM [the temperature of the cold envelope of Sgr B2(N), where propylene oxide has been detected, is arguably lower than 40 K[51]], such barriers become higher than RT, and that for T = 10 K, it is less than 1 meV, suggesting an effective trapping of the complex in the different potential wells. At a larger interaction distance, R = 4.0 Å (Fig. 6), the MEP becomes smoother with lower barriers separating the minima, making the passage from one minimum configuration to another easier, as confirmed by Fig. S1, reporting the energy profiles for fixed θ and ϕ values at increasing R distances, and because of the additional constraint, showing higher barriers than those corresponding to the MEP. Figure 6 also shows how the relative depth of the potential wells changes as a function of distance, that is, the global minimum might correspond to a different geometry (i.e., different values of θ and ϕ) as R changes. In light of the above considerations, this is found to have interesting consequences in the cold temperature regime: The anisotropic (orientation) dependence of the interaction components, rather than the absolute depth of the well, can be particularly effective in determining the most abundant configuration of the collision complex, which, once trapped in relative potential minima located at long and intermediate range, because of the barrier height, might not be able to interconvert to the global minimum at a shorter range.

The Ne–propylene oxide ILJ PES is also characterized by five minima, shown in Fig. 7 and Table IV, where the results of the present *ab initio* CCSD(T)/CBS calculations are also reported (the binding energies evaluated at each level of theory are reported in Table S2 of the supplementary material).

The interaction energies, due to the larger number of electrons of Ne, are sensibly higher, spanning the range from −18.05 to −14.47 meV. The comparison of the predicted ones with calculated *ab initio* minima again gives very close geometries for the five structures, although the energy differences might differ up to 3 meV and the ordering of the minima is slightly different. The global minimum on the ILJ PES corresponds to a configuration like that of He–propylene oxide at −18.05 meV interaction energy. *Ab initio* calculations, for the same geometry, rather predict a local minimum (−17.44 meV) very close in energy to the global one (−18.37 meV). It is worth noting that the lowest four minima in the ILJ surface do within less than 2 meV. The geometry of all minima is remarkably similar to that of He–propylene oxide, although the relative magnitude of the wells is different; however, as mentioned before, the

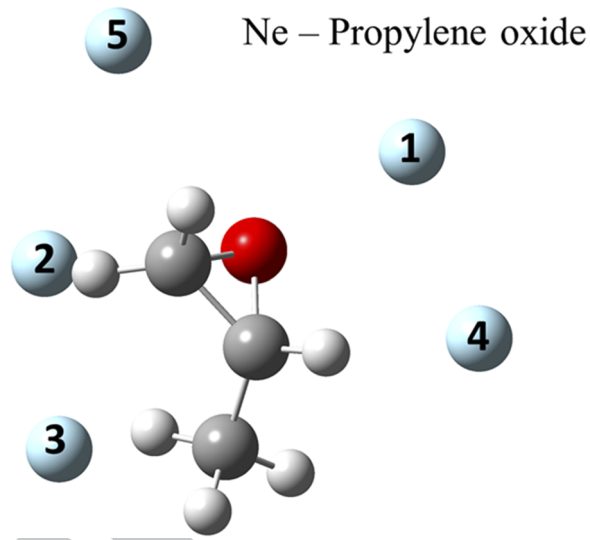

FIG. 7. Minimum geometries for Ne–propylene oxide identified on the ILJ PES. The numbering of the Ne atom corresponds to the minima reported in Table IV.

minima are so close in energy that the overall behavior is qualitatively the same. Blanco *et al.*[19,21] measured the rotational spectrum of Ne–propylene oxide and found that the most stable configuration (θ = 81° and 99°, ϕ = ±81° and ±99°, according to the reference coordinate system given in Ref. 21) is similar to minimum 3 found by us. The equilibrium distance between Ne and the center of mass of the molecule is 3.587 Å that is also comparable with the minima found by our model, as well as the dissociation energy, 11.4 meV, which is of the same order of the well depth (dissociation energy + zero-point energy) of the minima presented in this work (see Table IV).

Figures 8 and 9 show the contour maps of the potential energy surface for Ne–propylene oxide at R = 3.7 and 4.0 Å, respectively. The topology is similar to that of the He–propylene oxide system, with θ values larger than 130° characterized by a strongly repulsive potential and the minima to be found around the oxirane ring at values 40° < θ < 110°, spanning the whole range of ϕ. Figure S2 of the supplementary material shows the energy profiles for fixed θ and ϕ values at increasing R and clearly displays such behavior.

The MEP, reported in the right panel of Figs. 8 and 9, is characterized by higher barriers between the minima compared to He–propylene oxide. At R = 3.7 Å, there are three barriers and a small shoulder separating four minima, the higher ones of ~8–10 meV. Such a value is a factor of 2 larger than the corresponding one of He–propylene oxide and is expected to increase for homologous systems involving heavier Ng atoms. Therefore, in cold environments, these barriers can effectively trap the Ne–propylene oxide system in the different potential wells independently on their depth. As in the case of He–propylene oxide, by increasing the distance (see Fig. 9 at R = 4.0 Å and Fig. S2), the MEP becomes smoother and the barriers lower, although at correspondingly larger R values. Because of the higher barriers and the fact that the minima are comparable in energy, the above-mentioned effect

Author Proof

Published under an exclusive license by AIP Publishing

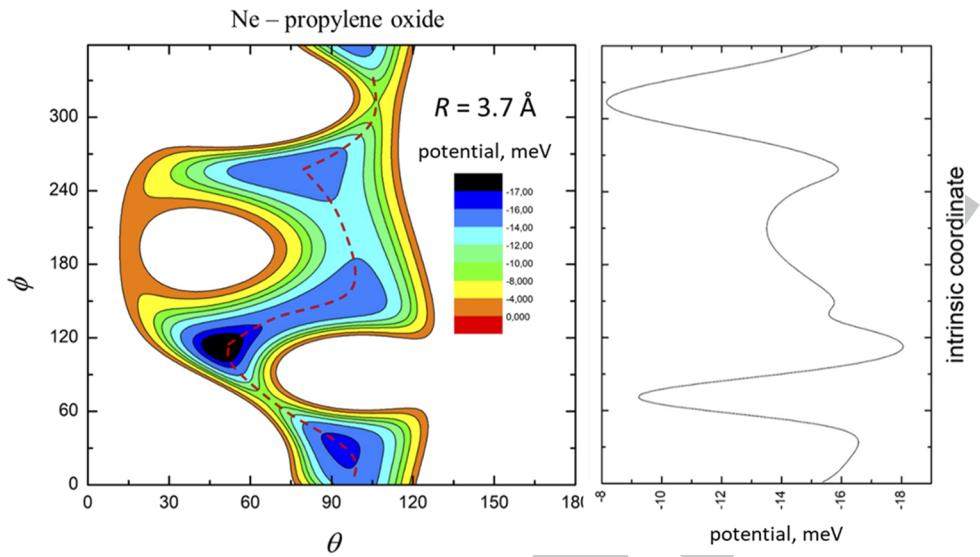

FIG. 8. The left panel shows the color contour map for the Ne–propylene oxide system at R = 3.7 Å. The axes report the angles θ and ϕ in degrees, while a color scale indicates the potential energy in meV. The red dashed line indicates the minimum energy path. The right panel shows the energy profile of the minimum energy path.

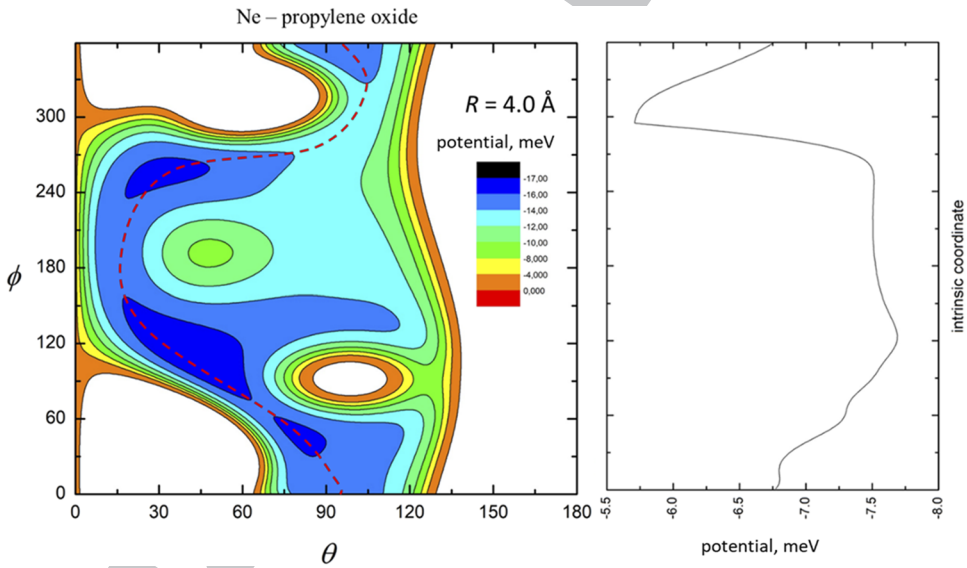

FIG. 9. The left panel shows the color contour map for the Ne–propylene oxide system at R = 4.0 Å. The axes report the angles θ and ϕ in degrees, while a color scale indicates the potential energy in meV. The red dashed line indicates the minimum energy path. The right panel shows the energy profile of the minimum energy path.

of a low-temperature dynamics, being determined by the trapping in the potential more attractive at a long range, rather than by their absolute depth at the equilibrium distance, might be emphasized with respect to the He–propylene oxide system.

V. FINAL REMARKS AND CONCLUSIONS

The results of gas-phase scattering experiments performed for the first time with a prototype chiral molecule are described here, accompanied by the observation of quantum interference effects in the two-body collisions: The integral cross sections for the scattering of He and Ne projectiles by the propylene oxide target have been measured as a function of noble gas velocity. The experiments have been performed with the MB technique, applied under high velocity and angular resolution conditions, to resolve the "glory" quantum interference effect. Measured cross sections probe in detail the strength, range, and anisotropy of projectile–target interaction at both long and intermediate intermolecular distances where the

Published under an exclusive license by AIP Publishing

potential wells are localized. The observed glory pattern exhibits for both systems an evident quenching of the amplitude due to the pronounced role of the interaction anisotropy emerging at intermediate separation distances.

For He–propylene oxide, cross sections measured at low velocity have been analyzed adopting an isotropic interaction, associated with an effective central field potential, while at high velocities, where the collision time significantly reduces and the probed distance R reduces, the data treatment required the IOSA adoption to account for the emerging role of the interaction anisotropy. For intermediate velocities, a combination of the two approaches has been adopted. For the Ne–propylene oxide collisions, the increased strength of the interaction anisotropy suggested the exclusive use of the IOSA method for the analysis of cross sections measured in the same velocity range.

The intermolecular interaction, considered of the van der Waals type, where size repulsion competes with dispersion attraction to define the resulting potential energy, has been formulated exploiting the ILJ function, whose parameters of zero-order value have been predicted on phenomenological ground. They have been anticipated exploiting the polarizability components of involved partners and subsequently adjusted, within restricted variation ranges, through the scattering data analysis. For He–propylene oxide, a direct comparison of the predicted PES minima with the results of previous[23] and new *ab initio* calculations permitted a further test and fine-tuning of the few parameters involved in the ILJ formulation. For Ne–propylene oxide, the parameters, simply scaled for the polarizability change when passing from He to Ne, provided a PES, tested on measured scattering data, whose predicted minima have been confirmed by the results of the present *ab initio* calculations.

The final potential parameters, reported in Tables I and II, allow a proper representation of the PES, whose analytical form emphasizes new details of the interaction that stimulate important considerations:

(1) The adopted method represents the intermolecular potential by an analytic formulation that makes use of a few parameters, with a well-defined physical meaning. This physically grounded restriction, at variance with most interpolation procedures, ensures the reliability of the interaction in the whole configuration space.

(2) The present method allows for a direct evaluation of the long-range dispersion coefficient C_6 that controls the capture character of the long-range forces and can be defined through the following sum:

$$C_6 = \sum_{i=1}^{4} n_i C_{6i},$$

where any partial C_{6i} contribution is obtained as $C_{6i} = \varepsilon \cdot r_m^6$ from the parameters reported in Tables I and II and n_i represents the number of interaction pairs of the same type.

(3) Both systems present a number of minima very close in energy so that the collision dynamics is likely to be determined from their overall contribution and from the possibility of interconversion between all of them.

(4) From the topography of the PES, the MEP can be evaluated, as shown in Sec. V, which provides the key information to evaluate the occurrence of adiabatic transitions between different configurations of the interacting systems. This represents a crucial point to properly assess the control of the collision dynamics selectivity under a variety of conditions.

(5) The energy barriers evaluated at each selected R as a function of polar angle, assuming fixed the other angle, appear significantly higher than those associated with the MEP.

(6) The location of the absolute minimum changes as the intermolecular distance varies, that is, the most stable configuration at a long range can substantially differ from that in the region of equilibrium distance. An important consequence is that the systems formed by the trapping from long-range anisotropic attractive forces can be channeled, during the relaxation of its internal degrees of freedom via fast nonadiabatic cooling, in configurations that can differ from that of the PES global minimum.

(7) The dissociation energy on Ne–propylene oxide estimated by Blanco *et al.*[19,21] is consistent with the well depth of the minima determined in the present work. Moreover, considerations made at point 6 can also be applied to this point.

(8) The formulation of the PES for Ar, Kr, Xe, and Rn–propylene oxide can be readily obtained by scaling the potential parameters for the different polarizability of the noble gas atom.

(9) Similarly, the same method can be applied, after parameter scaling for the change in polarizability, to the description of simple diatomic molecule–propylene oxide systems, when the diatom (H_2, N_2, and O_2), with rotational levels following a Boltzmann distribution at room and higher temperature, rotates sufficiently faster than propylene oxide, therefore behaving during the collision as a pseudo-atom interacting with propylene oxide with intermolecular forces basically of van der Waals nature. In particular, N_2 and O_2 would behave like Ar, as they show a similar isotropic polarizability component. Moreover, the marked anisotropic character of the intermolecular interaction emerges when the low temperature only allows the lower rotational levels of the diatoms to be populated. The complete potential formulation in this case must include the anisotropic contribution of the electrostatic components, as those due to permanent electric multipole interactions. The method can be extended to more complex systems, also of interest for their chiral properties, such as propylene oxide dimers.

(10) The obtained potential energy surfaces can be used to evaluate and investigate possible collision alignment processes, basic for chiral discrimination in gaseous streams and vortices in atmosphere environments.[5,52]

(11) The analytical formulation of the PES allows the calculation of physical, dynamical, and spectroscopic properties of the systems, which selectively depend on the weak anisotropic forces at both long and intermediate ranges of separation distances.

(12) It is also worth pointing out that the present methodology can be profitably used, as done here for the Ne–propylene oxide system, to preliminary address the search of stationary

Author Proof

Published under an exclusive license by AIP Publishing

points in multidimensional surfaces of increasing complexity, which can then be refined through high level calculations. Such a procedure is faster and strongly reduces the number of points to be evaluated *ab initio* on the PES to identify regions where minima or transition states are located. Moreover, its formulation allows us to obtain in an analytical form first and second derivates of the interaction with respect to radial and angular coordinates, related to force and force constants, speeding up their calculation in molecular dynamics simulations, where these quantities play a crucial role, and therefore alleviating the related computational burden.

SUPPLEMENTARY MATERIAL

The supplementary material contains tables of the binding energies for the investigated systems at different levels of theory. For these systems, plots of the energy profiles as a function of θ at fixed values of ϕ and vice versa, and the related discussion, are also provided.

ACKNOWLEDGMENTS

Federico Palazzetti acknowledges the Italian Ministry for Education, University and Research (MIUR) for financial support through SIR 2014, Scientific Independence of Young Researchers (Grant No. RBSI14U3VF).

AUTHOR DECLARATIONS

Conflict of Interest

Q6 ■.

DATA AVAILABILITY

The data that support the findings of this study are available within the article and its supplementary material.

REFERENCES

[1] B. A. McGuire, P. B. Carroll, R. A. Loomis, I. A. Finneran, P. R. Jewell, A. J. Remijan, and G. A. Blake, Science **352**, 1449–1452 (2016).
[2] F. Palazzetti, G. S. Maciel, A. Lombardi, G. Grossi, and V. Aquilanti, J. Chin. Chem. Soc. **59**, 1045–1052 (2013).
[3] V. Aquilanti, G. Grossi, A. Lombardi, G. S. Maciel, and F. Palazzetti, Phys. Scr. **78**, 058119 (2008).
[4] M. Quack, Angew. Chem., Int. Ed. Engl. **41**, 4618–4630 (2002).
[5] T.-M. Su, F. Palazzetti, A. Lombardi, G. Grossi, and V. Aquilanti, Rend. Fis. Acc. Lincei **24**, 291–297 (2013).
[6] J. D. Swalen and D. R. Herschbach, J. Chem. Phys. **27**, 100 (1957).
[7] D. R. Herschbach and J. D. Swalen, J. Chem. Phys. **29**, 761 (1958).
[8] R. W. Kawiecki, F. Devlin, P. J. Stephens, R. D. Amos, and N. C. Handy, Chem. Phys. Lett. **145**, 411–417 (1988).
[9] J. Šebestík and P. Bouř, J. Phys. Chem. Lett. **2**, 498–502 (2011).
[10] C. Merten, J. Bloino, V. Barone, and Y. Xu, J. Phys. Chem. Lett. **4**, 3424–3428 (2013).
[11] D.-C. Che, F. Palazzetti, Y. Okuno, V. Aquilanti, and T. Kasai, J. Phys. Chem. A **114**, 3280 (2010).
[12] D.-C. Che, K. Kanda, F. Palazzetti, V. Aquilanti, and T. Kasai, Chem. Phys. **399**, 180–192 (2012).
[13] S. Falcinelli, F. Vecchiocattivi, M. Alagia, L. Schio, R. Richter, S. Stranges, D. Catone, M. S. Arruda, L. A. V. Mendes, F. Palazzetti, V. Aquilanti, and F. Pirani, J. Chem. Phys. **148**, 114302 (2018).
[14] S. Falcinelli, M. Rosi, F. Pirani, D. Bassi, M. Alagia, L. Schio, R. Richter, S. Stranges, N. Balucani, V. Lorent, and F. Vecchiocattivi, Front. Chem. **7**, 621 (2019).
[15] F. Dubnikova and A. Lifshitz, J. Phys. Chem. A **104**, 4489–4496 (2000).
[16] M. Elango, G. S. Maciel, F. Palazzetti, A. Lombardi, and V. Aquilanti, J. Phys. Chem. A **114**, 9864–9874 (2010).
[17] A. N. Witt, Philos. Trans. R. Soc., A **359**, 1949–1959 (2001).
[18] B. A. McGuire, ApJS **239**, 17 (2018).
[19] S. Blanco, A. Maris, S. Melandri, and W. Caminati, Mol. Phys. **100**, 3245–3249 (2002).
[20] S. Blanco, A. Maris, A. Millemaggi, and W. Caminati, J. Mol. Struct. **612**, 309–313 (2002).
[21] S. Blanco, S. Melandri, A. Maris, W. Caminati, B. Velino, and Z. Kisiel, Phys. Chem. Chem. Phys. **5**, 1359–1364 (2003).
[22] Z. Su, N. Borho, and Y. Xu, J. Am. Chem. Soc. **128**, 17126–17131 (2006).
[23] A. Faure, P. J. Dagdigian, C. Rist, R. Dawes, E. Quintas-Sánchez, F. Lique, and M. Hochlaf, ACS Earth Space Chem. **3**, 964–972 (2019).
[24] B. Yang, P. Zhang, C. Qu, X. H. Wang, P. C. Stancil, J. M. Bowman, N. Balakrishnan, B. M. McLaughlin, and R. C. Forrey, J. Phys. Chem. A **122**, 1511–1520 (2018).
[25] Q. Hong, M. Bartolomei, F. Esposito, C. Coletti, Q. Sun, and F. Pirani, Phys. Chem. Chem. Phys. **23**, 15475–15479 (2021).
[26] K. B. Gubbels, S. Y. van der Meerakker, G. C. Groenenboom, G. Meijer, and A. van der Avoird, J. Chem. Phys. **136**, 074301 (2012).
[27] K. M. Walker, F. Dumouchel, F. Lique, and R. Dawes, J. Chem. Phys. **145**, 024314 (2016).
[28] A. Lombardi, F. Palazzetti, G. S. Maciel, V. Aquilanti, and M. B. Sevryuk, Int. J. Quantum Chem. **111**, 1651–1658 (2011).
[29] A. Lombardi and F. Palazzetti, "Chirality in molecular collision dynamics," J. Phys.: Condens. Matter **30**, 063003 (2018).
[30] F. Pirani and F. Vecchiocattivi, Mol. Phys. **45**, 1003–1013 (1982).
[31] F. Pirani, S. Brizi, L. F. Roncaratti, P. Casavecchia, D. Cappelletti, and F. Vecchiocattivi, Phys. Chem. Chem. Phys. **10**, 5489–5503 (2008).
[32] D. Cappelletti, M. Bartolomei, F. Pirani, and V. Aquilanti, J. Phys. Chem. A **106**, 10764–10772 (2002).
[33] D. Cappelletti, A. Bartocci, F. Grandinetti, S. Falcinelli, L. Belpassi, F. Tarantelli, and F. Pirani, Chem. Eur. J. **21**, 6234–6240 (2015).
[34] F. Pirani, D. Cappelletti, S. Falcinelli, D. Cesario, F. Nunzi, L. Belpassi, and F. Tarantelli, Angew. Chem., Int. Ed. **58**, 4195–4199 (2019).
[35] D. Cappelletti, A. Cinti, A. Nicoziani, S. Falcinelli, and F. Pirani, Front. Chem. **7**, 320 (2019).
[36] V. Aquilanti, G. Liuti, F. Pirani, F. Vecchiocattivi, and G. G. Volpi, J. Chem. Phys. **65**, 4751–4755 (1976).
[37] T. Nenner, H. Tien, and J. B. Fenn, J. Chem. Phys. **63**, 5439–5444 (1975).
[38] F. Pirani and F. Vecchiocattivi, J. Chem. Phys. **66**, 372–373 (1977).
[39] M. Child, *Molecular Collision Theory* (Clarendon Press, Oxford, 1974).
[40] F. Pirani, M. Albertí, A. Castro, M. Moix Teixidor, and D. Cappelletti, Chem. Phys. Lett. **394**, 37–44 (2004).
[41] M. Capitelli, D. Cappelletti, G. Colonna, C. Gorse, A. Laricchiuta, G. Liuti, S. Longo, and F. Pirani, Chem. Phys. **338**, 62–68 (2007).
[42] R. Cambi, D. Cappelletti, G. Liuti, and F. Pirani, J. Chem. Phys. **95**, 1852–1861 (1991).
[43] F. Pirani, D. Cappelletti, and G. Liuti, Chem. Phys. Lett. **350**, 286–296 (2001).
[44] T. N. Olney, N. M. Cann, G. Cooper, and C. E. Brion, Chem. Phys. **223**, 59–98 (1997).
[45] F. Nunzi, D. Cesario, L. Belpassi, F. Tarantelli, L. F. Roncaratti, S. Falcinelli, D. Cappelletti, and F. Pirani, Phys. Chem. Chem. Phys. **21**, 7330–7340 (2019).

Author Proof

Published under an exclusive license by AIP Publishing

Q9 [46] L. F. Roncarattti, L. Belpassi, D. Cappelletti, F. Pirani, and F. Tarantelli, J. Phys. Chem. A **113**, 15223–15232 (2009).
[47] A. L. de Araujo Oliveira, M. de Abreu Silva, F. Pirani, L. G. Machado de Macedo, and R. Gargano, Int. J. Quantum Chem. **120**, e26266 (2020).
Q10 [48] ■, Gaussian 09, Revision A.02, Gaussian, Inc., Wallingford, CT, 2016.
[49] K. A. Peterson, D. E. Woon, and T. H. Dunning, Jr., J. Chem. Phys. **100**, 7410 (1994).
[50] C. Coletti and N. Re, J. Phys. Chem. A **113**, 1578–1585 (2009).
[51] P. De Vicente and J. A. Martìn-Pintado, ASP Conf. Ser. **102**, 64–67 (1996).
[52] H.-N. Lee, L.-C. Chang, and T.-M. Su, Chem. Phys. Lett. **507**, 63–68 (2011).

Author Proof

Published under an exclusive license by AIP Publishing